

## Peroxynitrate and Peroxynitrite: A Complete Basis Set Investigation of Similarities and Differences between These NO<sub>x</sub> Species

Leif P. Olson,<sup>\*,†</sup> Michael D. Bartberger,<sup>‡,§</sup> and K. N. Houk<sup>\*,‡</sup>

Eastman Kodak Company, Research Laboratories, Rochester, New York 14650-1717, and  
Department of Chemistry and Biochemistry, University of California,  
Los Angeles, California 90095-1569

Received December 6, 2002; E-mail: leif.olson@kodak.com; houk@chem.ucla.edu

**Abstract:** Peroxynitric acid/peroxynitrate (PNA) rivals peroxynitrous acid/peroxynitrite (PNI) in importance as a reactive oxygen species. These species possess similar two-electron oxidative behavior. On the other hand, stark differences exist in the stability of these molecules as a function of pH and in the presence of CO<sub>2</sub>, and also in the types of bond homolysis reactions that PNA and PNI may undergo. Using CBS-QB3 theory, we examine these similarities and differences. The activation barriers for two-electron oxidation of NH<sub>3</sub>, H<sub>2</sub>S, and H<sub>2</sub>C=CH<sub>2</sub> by PNA and PNI are found to be generally similar. The O–O BDE of O<sub>2</sub>NOOCO<sub>2</sub><sup>−</sup> is predicted to be 26 kcal/mol greater than that of ONOOCO<sub>2</sub><sup>−</sup>. This accounts for the insensitivity of PNA to the presence of CO<sub>2</sub>. Likewise, the O–O BDE of O<sub>2</sub>NOOH is predicted to be 19 kcal/mol greater than that of ONOOH, in excellent agreement with experiment. The fundamental principle underlying the large differences in O–O BDEs between PNA and PNI species is that the NO<sub>2</sub> that is formed from PNI can relax from the <sup>2</sup>B<sub>2</sub> excited state to the <sup>2</sup>A<sub>1</sub> ground state, whereas no such comparable state change occurs with NO<sub>3</sub> from PNA. Decomposition of the anions O<sub>x</sub>NOO<sup>−</sup> is more complex, with the energetics influenced by solvation. ONOO<sup>−</sup> can homolyze to yield NO/O<sub>2</sub><sup>−</sup>; however, this pathway represents a thermodynamic “dead end” since the radical pairs generated by homolysis should mostly revert to starting material. However, decomposition of O<sub>2</sub>NOO<sup>−</sup> yields the stable products NO<sub>2</sub><sup>−</sup>/<sup>−</sup>O<sub>2</sub>, a couple that is more stable than starting material. This may occur either by initial formation of NO<sub>2</sub>/O<sub>2</sub><sup>−</sup> or NO<sub>2</sub><sup>−</sup>/<sup>−</sup>O<sub>2</sub>, with the latter intermediates thermodynamically favored both in the gas phase and in solution. Given the extremely fast back-reaction of the homolysis products, heterolysis probably dominates the observed O<sub>2</sub>NOO<sup>−</sup> decomposition kinetics. This is in agreement with the first of two “kinetically indistinguishable” mechanistic possibilities proposed for O<sub>2</sub>NOO<sup>−</sup> decomposition (Goldstein, S.; Czapski, G.; Lind, J.; Merényi, G. *Inorg. Chem.* **1998**, *37*, 3943–3947).

### Introduction

The chemical and biological properties of peroxynitrite (ONOO<sup>−</sup>, and peroxynitrous acid, ONOOH, collectively referred to here as PNI) have attracted great interest.<sup>1–3</sup> Recent studies of PNI have also revealed an important accompanying role of

peroxynitrate (O<sub>2</sub>NOO<sup>−</sup>, and peroxynitric acid, O<sub>2</sub>NOOH, collectively referred to here as PNA). This species almost invariably forms as a secondary product in many reactions of PNI.<sup>4</sup> Hence, the reactivity of PNI and PNA are closely intertwined, and PNA appears to have significance rivaling that of PNI.

Experimental studies of PNA and PNI reveal that although some aspects of these two superficially similar molecules are indeed not very different, there are situations where very disparate behavior is exhibited. For instance, PNA and PNI have rather similar pK<sub>a</sub> values<sup>1c,5</sup> and fairly similar two-electron reduction potentials,<sup>6</sup> but differ substantially in reactivity. At low pH, ONOOH is very unstable, readily undergoing O–O

\* Corresponding author.

† Eastman Kodak Company.

‡ Department of Chemistry and Biochemistry, University of California, Los Angeles.

§ Current address: Department of Molecular Structure and Design, Amgen Inc., One Amgen Center Drive, M/S 29-M–B, Thousand Oaks, California 91320.

- (1) For recent reviews on peroxynitrite chemistry, see: (a) Beckman, J. S.; Koppenol, W. H. *Am. J. Physiol. (Cell Physiol.)* **1996**, *271*, C1424–C1437. (b) Edwards, J. O.; Plumb, R. C. *Prog. Inorg. Chem.* **1994**, *33*, 599–635. (c) Pryor, W. A.; Squadrito, J. L. *Am. J. Physiol. (Lung Cell. Mol. Physiol.)* **1995**, *268*, L699–L722. (2) (a) Kaur, H.; Halliwell, B. *FEBS Lett.* **1994**, *350*, 9–12. (b) Matheis, G.; Sherman, M. P.; Buckberg, G. D.; Haybron, D. M.; Young, H. H.; Ignarro, L. J. *Am. J. Physiol. (Heart Circ. Physiol.)* **1992**, *262*, H616–H620. (c) White, R. C.; Brock, T. A.; Chang, L. Y.; Crapo, J.; Briscoe, P.; Ku, D.; Bradley, W. A.; Gianturco, S. H.; Gore, J.; Freeman, B. A.; Tarpey, M. M. *Proc. Natl. Acad. Sci. U.S.A.* **1994**, *91*, 1044–1048. (d) Dawson, V. L.; Dawson, T. M.; London, E. D.; Bredt, D. S.; Snyder, S. H. *Proc. Natl. Acad. Sci. U.S.A.* **1991**, *88*, 6368–6371.

- (3) (a) Padmaja, S.; Squadrito, G. L.; Lemercier, J. N.; Cueto, R.; Pryor, W. A. *Free Radical Biol. Med.* **1996**, *21*, 317–322. (b) Pryor, W. A.; Jin, X.; Squadrito, G. L. *Proc. Natl. Acad. Sci. U.S.A.* **1994**, *91*, 11 173–11 177. (c) Beckman, J. S.; Ischiropoulos, H.; Zhu, L.; Van der Woerd, M.; Smith, C.; Chen, J.; Harrison, J.; Martin, J. C.; Tsai, M. *Arch. Biochem. Biophys.* **1992**, *298*, 438–445. (4) (a) Goldstein, S.; Czapski, G. *J. Am. Chem. Soc.* **1998**, *120*, 3458. (b) Hodges, G. R.; Ingold, K. U. *J. Am. Chem. Soc.* **1999**, *121*, 10 695. (5) (a) Kissner, R.; Nauser, T.; Bugnon, P.; Lye, P. G.; Koppenol, W. H. *Chem. Res. Toxicol.* **1997**, *10*, 1285–1292. (b) Løgager, T.; Sehested, K. *J. Phys. Chem.* **1993**, *97*, 10 047–10 052. (c) Goldstein, S.; Czapski, G. *Inorg. Chem.* **1997**, *36*, 4156–4162.

homolysis to give the OH/NO<sub>2</sub> radical pair.<sup>7</sup> Conversely, O<sub>2</sub>-NOOH is relatively stable at moderate to low pH.<sup>4</sup> Under these conditions, very little O–O homolysis of O<sub>2</sub>NOOH occurs, but a slow N–O bond cleavage reaction to give the OOH/NO<sub>2</sub> radical pair occurs.

At higher pH, the order of stability of PNA and PNI are reversed. ONOO<sup>−</sup> is fairly stable, decomposing only slowly to yield NO<sub>2</sub><sup>−</sup> and <sup>3</sup>O<sub>2</sub>,<sup>7a,b</sup> by a higher order mechanism. In contrast, O<sub>2</sub>NOO<sup>−</sup> decomposes relatively rapidly to NO<sub>2</sub><sup>−</sup> and <sup>3</sup>O<sub>2</sub>, either by a mechanism involving homolysis to yield NO<sub>2</sub><sup>−</sup>/O<sub>2</sub><sup>−</sup>, or by heterolysis to yield initially <sup>1</sup>O<sub>2</sub>/NO<sub>2</sub><sup>−</sup>.<sup>6a,c,8</sup> CO<sub>2</sub> greatly destabilizes ONOO<sup>−</sup>, however,<sup>9</sup> as its adduct, ONO-OCO<sub>2</sub><sup>−</sup>, forms readily and undergoes fairly rapid homolysis to give NO<sub>2</sub> + CO<sub>3</sub><sup>−</sup>.<sup>10</sup> This adduct possesses an even weaker O–O bond than ONOOH.<sup>6</sup> On the other hand, PNA is known to be insensitive to the presence of CO<sub>2</sub>.<sup>4</sup> These differences in homolytic and heterolytic activity of the nitrogen oxides are important factors in atmospheric chemistry as well as biological chemistry.<sup>11</sup>

Quantum mechanical calculations have been successful in predicting and rationalizing various aspects of PNI reactivity. For example, the experimentally observed rearrangement of ONOOH to HNO<sub>3</sub> was predicted by B3LYP/6-31G\* density functional theory (DFT) calculations to occur by facile O–O homolysis,<sup>12</sup> followed by N–O recombination, rather than an energetically demanding concerted pathway.<sup>13</sup> This prediction of a stepwise pathway has been verified by experimental studies in which the OH/NO<sub>2</sub> radical pair intermediate has been detected.<sup>14</sup> DFT calculations at this level also predicted that ONOOH should be capable of oxidizing sulfides to sulfoxides and alkenes to epoxides, and both of these predictions have been confirmed experimentally.<sup>15</sup> The observed destabilizing effect of CO<sub>2</sub> on ONOO<sup>−</sup> was also rationalized by DFT calculations

of the O–O BDE of ONOOCO<sub>2</sub><sup>−</sup>, which indicated a very facile O–O bond homolysis<sup>12</sup> to give NO<sub>2</sub> + CO<sub>3</sub><sup>−</sup>.

In this paper, we utilize high-accuracy ab initio methodology to compare and contrast the reactivity of PNI and PNA. We find that PNI and PNA should behave similarly in two-electron oxidations involving O-atom transfer reactions with oxidizable substrates. On the other hand, the O–O bond homolysis reactions of O<sub>x</sub>NOOR (x = 1 or 2, R = H or CO<sub>2</sub><sup>−</sup>) are much more facile when x = 1 than when x = 2, both in the well-known case when R = H, and also when R = CO<sub>2</sub><sup>−</sup>. This difference can be explained using a combination of quantum mechanics and thermochemical data, in terms of the differing reorganization energies<sup>19</sup> of the NO<sub>2</sub> and NO<sub>3</sub> radicals which are formed upon O–O homolysis. Our calculations serve to demonstrate and rationalize why homolytic or heterolytic mechanisms for O<sub>2</sub>NOO<sup>−</sup> are both reasonably facile, unlike ONOO<sup>−</sup> heterolysis (a thermodynamically nonviable pathway) or homolysis (a thermodynamic dead end).

## Computational Methods

All calculations were done using Gaussian 98<sup>16a</sup> Bond dissociation energies (BDEs) for homolytic reactions of PNI and PNA, along with transition structures for several representative oxidation reactions of these species were located using the Complete Basis Set (CBS-QB3) methodology of Petersson et al.<sup>17</sup> This level of theory has been shown to give excellent results in reproducing the heats of formation of a number of small organic and inorganic molecules (the G2 test set)<sup>18</sup> for which accurate thermochemical data are known, with bond dissociation energies typically accurate to within 2 kcal/mol of experiment.<sup>17</sup>

On the basis of general expectations of fast recombination rates for unhindered radicals, as well as the known high second-order rate constants for the various recombination reactions of HO•, NO<sub>2</sub>•, CO<sub>3</sub><sup>−</sup>, and similar radicals in solution,<sup>14</sup> it is reasonable to correlate our calculated BDEs with activation barriers to homolytic dissociation.

Solvation energies were evaluated using the PCM method of Tomasi<sup>16b–d</sup> at the PCM/B3LYP/6-311+G\*//B3LYP/6-311G\* level. In some cases, these solvation corrections were applied to the CBS-QB3 BDEs.

## Results and Discussion

**O-Atom Transfer Reactions from PNI and PNA to NH<sub>3</sub>, H<sub>2</sub>S, and H<sub>2</sub>C=CH<sub>2</sub>.** Figure 1 depicts our computed transition

- (6) (a) Merenyi, G.; Lind, J. *Chem. Res. Toxicol.*, **1998**, *11*, 243. (b) Merenyi, G.; Lind, J.; Goldstein, S.; Czapski, G. *Chem. Res. Toxicol.* **1998**, *11*, 712–713. (c) Goldstein, S.; Czapski, G.; Lind, J.; Merenyi, G. *Inorg. Chem.* **1998**, *37*, 3943–3947.
- (7) Studies mostly supporting a radical mechanism for ONOOH decomposition: (a) Gerasimov, O. V.; Lymar, S. V. *Inorg. Chem.* **1999**, *38*, 4317–4321. (b) Coddington, J. W.; Hurst, J. K.; Lymar, S. V. *J. Am. Chem. Soc.* **1999**, *121*, 2438. (c) Squadrito, G. L.; Pryor, W. A. *Chem. Res. Toxicol.* **1998**, *11*, 718–719. (d) Radi, R. *Chem. Res. Toxicol.* **1998**, *11*, 720–721. (e) Richeson, C. E.; Mulder, P.; Bowry, V. W.; Ingold, K. U. *J. Am. Chem. Soc.* **1998**, *120*, 7211–7219. (f) Goldstein, S.; Meyerstein, D.; van Eldik, R.; Czapski, G. *J. Phys. Chem. A* **1999**, *103*, 6587–6590. (g) A dissenting viewpoint: Padmaja, S.; Kissner, R.; Bounds, P. L.; Koppenol, W. H. *Helv. Chim. Acta* **1998**, *81*, 1201. (h) Koppenol, W. H. *Chem. Res. Toxicol.* **1998**, *11*, 716–717.
- (8) Regimbal, J.-M.; Mozurkewich, M. *J. Phys. Chem.* **1997**, *101*, 8822–8829.
- (9) (a) Uppu, R. M.; Pryor, W. A. *J. Am. Chem. Soc.* **1999**, *121*, 9738–9739. (b) Lemerrier, J.-N.; Padmaja, S.; Cueto, R.; Squadrito, G. L.; Uppu, R. M.; Pryor, W. A. *Arch. Biochem. Biophys.* **1997**, *345*, 160–170. (c) Gow, A.; Duran, D.; Thom, S. R.; Ischiropoulos, H. *Arch. Biochem. Biophys.* **1996**, *333*, 42–48.
- (10) Studies supporting a radical mechanism for ONOOCO<sub>2</sub><sup>−</sup> decomposition: (a) Goldstein, S.; Czapski, G. *J. Am. Chem. Soc.* **1999**, *121*, 2444. (b) Lymar, S. V.; Hurst, J. K. *Chem. Res. Toxicol.* **1998**, *11*, 714–715. (g) Koppenol, W. H. *Chem. Res. Toxicol.* **1998**, *11*, 716–717.
- (11) Jitariu, L. C.; Hirst, D. M. *J. Phys. Chem. A* **1999**, *103*, 6673, and references therein. These authors studied the reaction of NO<sub>3</sub>• and HO• in the context of atmospheric chemistry, using “G2MP2\*”, their modified version of G2MP2 theory (ref 18).
- (12) Houk, K. N.; Condroski, K. R.; Pryor, W. A. *J. Am. Chem. Soc.* **1996**, *118*, 13 002.
- (13) Koppenol, W. H.; Moreno, J. J.; Pryor, W. A.; Ischiropoulos, H.; Beckman, J. S. *Chem. Res. Toxicol.* **1992**, *5*, 834–842.
- (14) (a) Goldstein, S.; Saha, A.; Lymar, S. V.; Czapski, G. *J. Am. Chem. Soc.* **1998**, *120*, 5549, and references therein. (b) Merenyi, G.; Lind, J.; Goldstein, S.; Czapski, G. *J. Phys. Chem. A* **1999**, *103*, 5685–5691, and references therein.
- (15) Experimentally, oxygen transfer from ONOOH to alkenes has been found to be a slow reaction, but the oxidation of organic sulfides is fast: Vayssié, S.; Elias, H. *Angew. Chem. Int. Ed.* **1998**, *37*, 2088.

- (16) (a) All calculations were performed using Gaussian: Frisch, M. J.; Trucks, G. W.; Schlegel, H. B.; Scuseria, G. E.; Robb, M. A.; Cheeseman, J. R.; Zakrzewski, V. G.; Montgomery, J. A., Jr.; Stratmann, R. E.; Burant, J. C.; Dapprich, S.; Millam, J. M.; Daniels, A. D.; Kudin, K. N.; Strain, M. C.; Farkas, O.; Tomasi, J.; Barone, V.; Cossi, M.; Cammi, R.; Mennucci, B.; Pomelli, C.; Adamo, C.; Clifford, S.; Ochterski, J.; Petersson, G. A.; Ayala, P. Y.; Cui, Q.; Morokuma, K.; Malick, D. K.; Rabuck, A. D.; Raghavachari, K.; Foresman, J. B.; Cioslowski, J.; Ortiz, J. V.; Stefanov, B. B.; Liu, G.; Liashenko, A.; Piskorz, P.; Komaromi, I.; Gomperts, R.; Martin, R. L.; Fox, D. J.; Keith, T.; Al-Laham, M. A.; Peng, C. Y.; Nanayakkara, A.; Gonzalez, C.; Challacombe, M.; Gill, P. M. W.; Johnson, B. G.; Chen, W.; Wong, M. W.; Andres, J. L.; Head-Gordon, M.; Replogle, E. S.; Pople, J. A. *Gaussian 98*, revision A.9; Gaussian, Inc.: Pittsburgh, PA, 1998. (b) Miertus, S.; Scrocco, E.; Tomasi, J. *Chem. Phys.* **1981**, *55*, 117. (c) Miertus, S.; Tomasi, J. *Chem. Phys.* **1982**, *65*, 239. (d) Cossi, M.; Barone, V.; Cammin, R.; Tomasi, J. *Chem. Phys. Lett.* **1996**, *255*, 327.
- (17) (a) Montgomery, J. A.; Frisch, M. J.; Ochterski, J. W.; Petersson, G. A. *J. Chem. Phys.* **1999**, *110*, 2822. (b) Petersson, G. A.; Tensfeldt, T. G.; Montgomery, J. A. *J. Chem. Phys.* **1991**, *94*, 6091. (c) Ochterski, J. W.; Petersson, G. A.; Montgomery, J. A. *J. Chem. Phys.* **1996**, *104*, 2598.
- (18) Curtiss, L. A.; Raghavachari, K.; Trucks, G. W.; Pople, J. A. *J. Chem. Phys.* **1991**, *94*, 7221.
- (19) McKee, M. L. *J. Am. Chem. Soc.* **1995**, *117*, 1629.

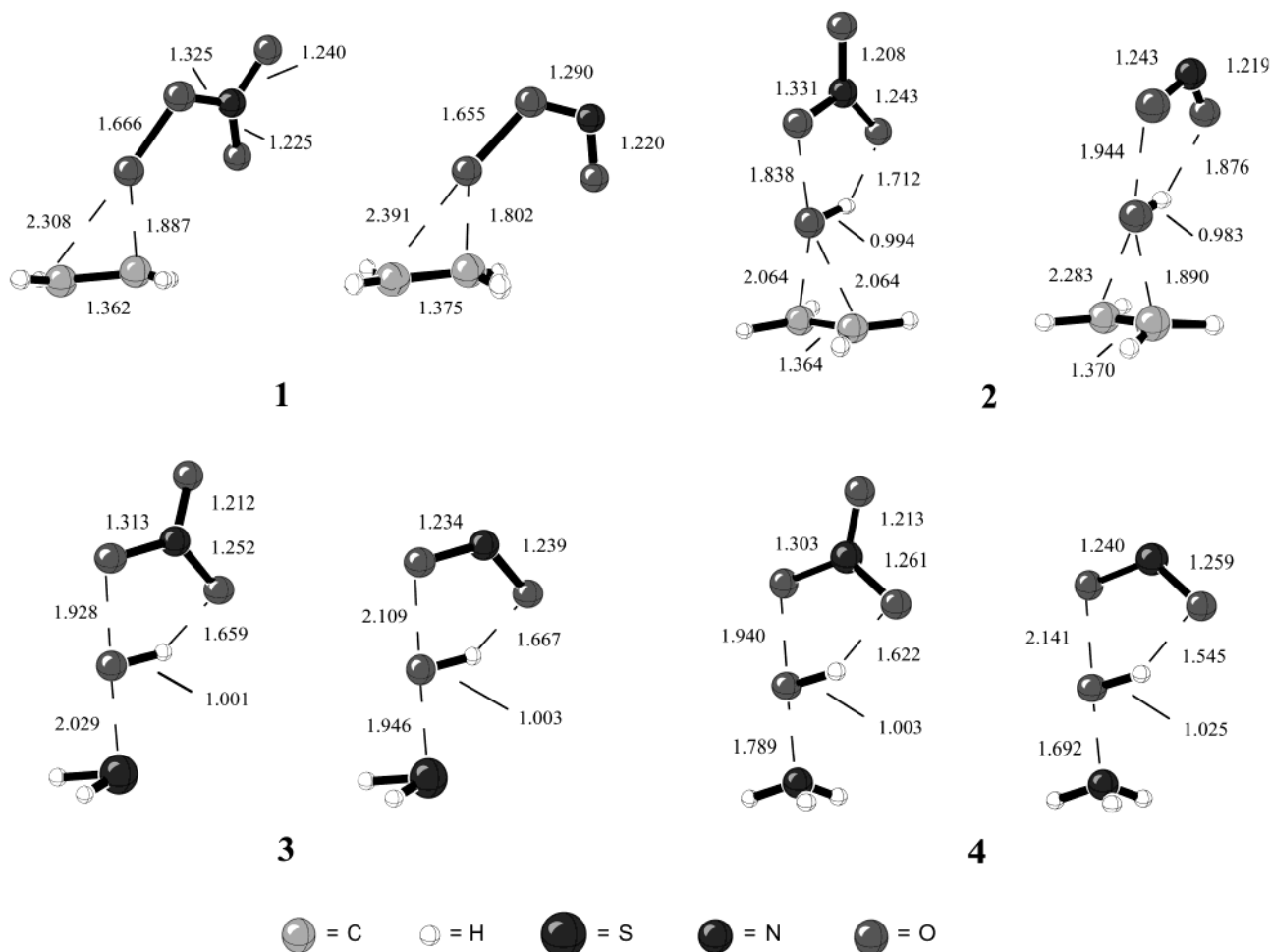
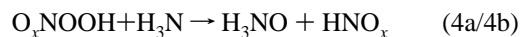
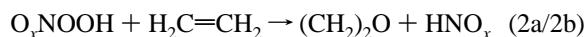
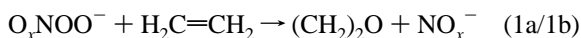


**Figure 1.** CBS-QB3 computed transition structures for several oxidation reactions of PNA and PNI.

structures at the CBS-QB3 level for oxidations of  $\text{NH}_3$ ,  $\text{H}_2\text{S}$ , and  $\text{H}_2\text{C}=\text{CH}_2$  by PNA and PNI. As found previously for the oxidations by PNI at the density functional theory (B3LYP/6-31G\*) level,<sup>12</sup> the reactions of the neutral peroxides involve mainly OH transfer, with proton transfer occurring after the transition state. This resembles results for both peroxynitrous acid and percarboxylic acids.<sup>12,21,22,23,24a</sup> The reactions of the anionic peroxides with  $\text{H}_2\text{C}=\text{CH}_2$  possess transition states corresponding to nucleophilic attack of  $\text{O}_x\text{NOO}^-$ , with asynchronous formation of the two C–O bonds. The nucleophilic attack transition state structure in these cases is reminiscent of the B3LYP/6-31G\* transition state for O-atom transfer to the carbonyl group of acetone by peroxynitrite<sup>24b</sup> (or peroxynitrate<sup>24c</sup>) ion, to yield dimethyldioxirane and nitrite (or nitrate) ion<sup>24d</sup>



From the computed activation barriers (Table 1) it is predicted that the 2-electron oxidative capacities of PNA and PNI are

**Table 1.** Comparison of CBS-QB3 Computed Energy Barriers for PNA and PNI

PNI reaction	$\Delta E$ (ts–gs)	PNA reaction	$\Delta E$ (ts–gs)
<b>1a</b>	14.7	<b>1b</b>	13.6
<b>2a</b>	17.1	<b>2b</b>	19.6
<b>3a</b>	20.9	<b>3b</b>	20.6
<b>4a</b>	20.6	<b>4b</b>	23.5

Energies in kcal/mol.

verysimilar. For this set of reactions, the structural and energetic similarities in the transition structures for oxygen transfer by PNA and PNI outweigh minor differences.

**Computed O–O and N–O BDEs for  $\text{O}_x\text{NOOR}$  ( $x = 1$  or  $2$ ,  $\text{R} = \text{H}$  or  $\text{CO}_2^-$ ).** In contrast to the oxygen atom transfer reactions, the bond dissociation energies (BDEs) for the O–O homolysis reactions of PNA and PNI are very different. Computed homolysis and heterolysis energies of  $\text{O}_x\text{NOOR}$  and  $\text{O}_x\text{NOO}^-$  ( $x = 1$  or  $2$ ,  $\text{R} = \text{H}$  or  $\text{CO}_2^-$ ) are given in Table 2 and are discussed below.

(20) Curtiss, L. A.; Raghavachari, K.; Redfern, P. C.; Rassolov, V.; Pople, J. A. *J. Chem. Phys.* **1998**, *109*, 7764.

(21) Houk, K. N.; Liu, J.; DeMello, N. C.; Condroski, K. *J. Am. Chem. Soc.* **1997**, *119*, 10 147–10 152.

(22) Bach, R. D.; Glukhovtsev, M. N.; Canepa, C. *J. Am. Chem. Soc.* **1998**, *120*, 775–783.

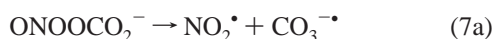
(23) Bach, R. D.; Glukhovtsev, M. N.; Gonzalez, C.; Marquez, M.; Estevez, C. M.; Baboul, A. G.; Schlegel, H. B. *J. Phys. Chem. A* **1997**, *101*, 6092–6100.

**Table 2.** Computed Energies (CBS-QB3) of Single-Bond Dissociation Reactions in Figure 2

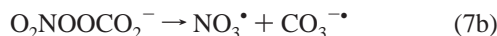
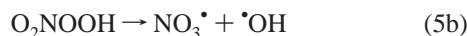
reaction	$\Delta E_{rxn}$	reaction	$\Delta E_{rxn}$
<b>5a</b>	19.7	<b>5b</b>	39.0
<b>6a</b>	27.9	<b>6b</b>	24.8
<b>7a</b>	7.5	<b>7b</b>	33.2
<b>8a</b>	28.5	<b>8b</b>	31.8
<b>9a</b>	18.3	<b>9b</b>	17.7

Energies in kcal/mol.

Peroxynitrous acid possesses an O–O BDE of only 20 kcal/mol (eq **5a**), and the peroxynitrite-CO<sub>2</sub> adduct possesses an O–O BDE of only 8 kcal/mol (eq **7a**)



However, O–O bond homolysis values rise to 39 kcal/mol (experimental value 39.6 kcal/mol)<sup>11</sup> and 33 kcal/mol for the corresponding nitro compounds (eqs **5b** and **7b**)



These calculations are consistent with a picture where O<sub>2</sub>NOOH and O<sub>2</sub>NOOCO<sub>2</sub><sup>−</sup> are reasonably stable peroxides, whereas ONOOH (and especially ONOOCO<sub>2</sub><sup>−</sup>) should be highly reactive toward O–O homolysis.

O<sub>2</sub>NOOCO<sub>2</sub><sup>−</sup> is the product of the reaction of O<sub>2</sub>NOO<sup>−</sup> with CO<sub>2</sub>. Calculations (B3LYP/6-31G\*) indicate that there is no gas-phase barrier to the formation of O<sub>2</sub>NOOCO<sub>2</sub><sup>−</sup> from peroxynitrate and CO<sub>2</sub>, as is the case with ONOOCO<sub>2</sub><sup>−</sup>.<sup>12</sup> CBS-QB3 energies of CO<sub>2</sub> adduct formation are similarly exothermic for both O<sub>x</sub>NOO<sup>−</sup> species, ca. 17–18 kcal/mol (eqs **9a** and **9b**)



The weakest bond in O<sub>2</sub>NOOH is not the O–O bond (eq **5b**); rather, it is the N–O bond (eq **6b**), with a computed BDE of 24.8 kcal/mol. (Previous “G2MP2\*” calculations predict an N–O BDE of 27.8 kcal/mol).<sup>11</sup> Although this bond is of about the same strength as the comparable N–O bond in ONOOH (eq **6a**; BDE = 27.9 kcal/mol)



the lack of a favorable O–O homolysis pathway for O<sub>2</sub>NOOH

(24) (a) Bartberger, M. D.; Olson, L. P.; Houk, K. N. *Chem. Res. Toxicol.* **1998**, *11*, 710–711. (b) Yang, D.; Tang, Y.-C.; Chen, J.; Wang, X.-C.; Bartberger, M. D.; Houk, K. N.; Olson, L. P. *J. Am. Chem. Soc.* **1999**, *121*, 11 976–11 983. (c) Olson, L. P. unpublished results; B3LYP/6-31G\* relative energies and geometries for O<sub>2</sub>NOO<sup>−</sup> oxidation of acetone are very similar to those for ONOO<sup>−</sup> oxidation of acetone as in Reference 24b. (d) Although DFT theory finds transition states for the gas-phase reaction of peroxynitrite ion or peroxynitrous acid with a ketone to yield a dioxirane, some recent pulse radiolysis experiments do not find evidence of dioxirane formation in aqueous solution: Merenyi, G.; Lind, J.; Goldstein, S. *J. Am. Chem. Soc.* **2002**, *124*, 40–48.

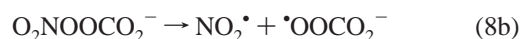
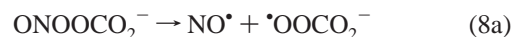
**Table 3.** Computed Energies (CBS-QB3) of Single-Bond Dissociation Reactions in Figure 3

reaction	$\Delta E_{rxn}$	reaction	$\Delta E_{rxn}$
<b>10a</b>	32.4	<b>10b</b>	36.3
<b>11a</b>	95.6	<b>11b</b>	22.8
<b>12a</b>	42.7	<b>12b</b>	−5.9

Energies in kcal/mol.

means that the expected products of homolysis in this case are OOH + NO<sub>2</sub>, rather than OH + NO<sub>3</sub>.<sup>6c,8,11</sup>

Likewise, another decomposition pathway for ONOOCO<sub>2</sub><sup>−</sup> and O<sub>2</sub>NOOCO<sub>2</sub><sup>−</sup> is N–O homolysis (eqs **8a** and **8b**)



These N–O homolyses are energetically similar, requiring 29–32 kcal/mol (Table 2). However, in the case of ONOOCO<sub>2</sub><sup>−</sup>, homolysis of the N–O bond (eq **8a**) should constitute an insignificant decomposition pathway for ONOOCO<sub>2</sub><sup>−</sup>, as O–O homolysis (8 kcal/mol, eq **7a**) will clearly predominate.

For O<sub>2</sub>NOOCO<sub>2</sub><sup>−</sup>, an O–O homolysis pathway (eq **7b**) is less favorable at 33.2 kcal/mol, although competitive with N–O homolysis (31.8 kcal/mol, eq **8b**). Due to the relatively weak (17.7 kcal/mol) O–C bond in O<sub>2</sub>NOOCO<sub>2</sub><sup>−</sup>, (eq **9b**), an equilibrium between O<sub>2</sub>NOO<sup>−</sup> + CO<sub>2</sub> and O<sub>2</sub>NOOCO<sub>2</sub><sup>−</sup> is likely to exist (especially because of hydration of dissolved CO<sub>2</sub>)



Decarboxylation should be somewhat facile, and PNA will self-decompose via the anion O<sub>2</sub>NOO<sup>−</sup>.

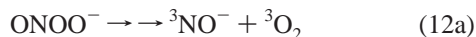
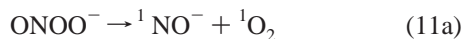
We also explored the influence of aqueous solvation on these reactions using the PCM solvation model. In the reactions involving neutral species and N–O and O–O homolysis of PNA and PNI CO<sub>2</sub> adducts, solvation has little effect on the relative energies. For example, the energy required for cleavage of the O–O bond is still found to be ca. 21 kcal/mol greater for O<sub>2</sub>NOOCO<sub>2</sub><sup>−</sup> (O–O BDE 33 kcal/mol, eq **7a**) than for ONOOCO<sub>2</sub><sup>−</sup> (O–O BDE 8 kcal/mol, eq **7b**). Energetics of O–O cleavage in the neutral acids HOONO and HOONO<sub>2</sub> (eqs **5a** and **5b**) each change by less than 2 kcal/mol, as the effect of solvation on neutral radicals is generally small.

**Relative Stabilities of O<sub>x</sub>NOO<sup>−</sup> Species (x = 1 or 2).** In the absence of Brønsted or Lewis acids, the decomposition of O<sub>2</sub>NOO<sup>−</sup> in aqueous solution is observed to be faster than decomposition of ONOO<sup>−</sup>.<sup>6a,c,8</sup> Interestingly, the products of decomposition in either case are NO<sub>2</sub><sup>−</sup> and <sup>3</sup>O<sub>2</sub>.

For ONOO<sup>−</sup>, a simple bond cleavage mechanism seems unlikely, as the stoichiometry is inconsistent with the observed products. Indeed, ONOO<sup>−</sup> decomposition is thought to be a relatively complicated process.<sup>7a,b</sup> Nonetheless, the simple bond cleavage reactions **10a–12a** (Table 3) do provide an interesting

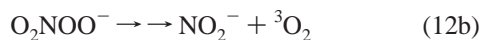
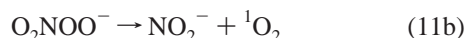


comparison to the parallel set of reactions of  $\text{O}_2\text{NOO}^-$



Reaction **10a** is simply the reverse of the well-known diffusion-controlled reaction of nitric oxide and superoxide to form peroxynitrite ( $-\mathbf{10a}$ ).<sup>1</sup> There are two other possible pathways for N–O bond breaking, both of which obey spin conservation: reaction **11a** to yield singlet nitroxyl anion and singlet oxygen, or reaction **12a** to yield (singlet-coupled) triplet nitroxyl anion and triplet oxygen. Because both products from **11a** are formed in excited states, this reaction is quite disfavored at >90 kcal/mol, and despite one report in support of this pathway,<sup>26a</sup> it has since been ruled out.<sup>26b</sup> Reaction **12a** yields these products in the ground state, so is not as severely disfavored as **11a**; however, this reaction is still 10 kcal/mol more endothermic than **10a**. Furthermore, even though the endothermicities of both **10a** and **12a** are computed to be lower in water, reaction **10a** is favored even more strongly. After aqueous solvation calculations, reaction **10a** is +20.0 kcal/mol, whereas **12a** is +33.8 kcal/mol, an even larger difference than that of the gas-phase values (Table 3). Although **10a** is clearly the most favored N–O bond breaking mechanism for  $\text{ONOO}^-$ , it is important to note that this is still an endothermic reaction (with a diffusion controlled rate for the back reaction  $-\mathbf{10a}$ ) and therefore seemingly represents a thermodynamic “dead end” in the absence of some efficient pathway for further reaction of products. The enzyme superoxide dismutase (SOD) can “detect”  $\text{ONOO}^-$  undergoing reaction **10a**, by efficiently catalyzing the disproportionation of superoxide such that it becomes competitive with recombination of superoxide and nitric oxide.<sup>1c</sup>

The mechanism for decomposition of  $\text{O}_2\text{NOO}^-$  is probably less complicated than the  $\text{ONOO}^-$  mechanism, but key details have still been unclear. The observed net reaction **12b** has been proposed to occur by either the homolysis reaction **10b** followed by electron transfer, or the heterolysis reaction **11b** followed by singlet to triplet relaxation of  $\text{O}_2$  (or a combination of both pathways)<sup>6c</sup>



The key difference between  $\text{O}_2\text{NOO}^-$  and  $\text{ONOO}^-$  is that, largely due to the stability of  $\text{NO}_2^-$ , the overall reaction **12b** is exothermic (Table 3). This provides a driving force for N–O bond breaking even in the absence of a trapping agent, thereby allowing a relatively straightforward decomposition pathway.

All that it is required for  $\text{O}_2\text{NOO}^-$  to be unstable is that **10b** and/or **11b** are not too highly endothermic, and that electron transfer is competitive with  $-\mathbf{10b}$  and/or spin inversion of dioxygen is competitive with  $-\mathbf{11b}$ . Goldstein et al. studied the effect of a variety of trapping agents for superoxide and nitrogen dioxide on the observed rate of decomposition of  $\text{O}_2\text{NOO}^-$ ;<sup>6c</sup> however, it could not be fully determined to what extent either reaction participates in uncatalyzed  $\text{O}_2\text{NOO}^-$  decomposition. Therefore, two kinetically equivalent schemes were proposed for  $\text{O}_2\text{NOO}^-$  decomposition: in the first case, **10b** and **11b** should have very similar forward rate constants but **11b** would dominate the kinetics because  $-\mathbf{10b}$  is very fast (but  $-\mathbf{11b}$  might be slower); in the second case, essentially all reaction would be via **10b**, with radical cage effects invoked to permit electron transfer to compete with  $-\mathbf{10b}$ .

The thermodynamic computations indicate that reaction **11b** is significantly less endothermic than **10b** (22.8 vs 36.3 kcal/mol), which would tend to indicate a larger rate constant for **11b**. However, solvation greatly reduces the magnitude of the difference, with **10b** endothermic by 19.4 kcal/mol and **11b** endothermic by 17.7 kcal/mol. This is a result of relatively favorable solvation of superoxide compared to nitrite. Although the SCRF solvation energy corrections are not expected to be quantitatively accurate (the experimental  $E_a$  for decomposition of  $\text{O}_2\text{NOO}^-$  in water is found to be  $25.2 \pm 0.4$  kcal/mol at pH 8.9),<sup>6c,27</sup> this result is in better agreement with the first of Goldstein et al.’s kinetically indistinguishable mechanisms for  $\text{O}_2\text{NOO}^-$  decomposition, in which **10b** and **11b** are competitive.<sup>6c</sup> It is in poorer agreement with the second mechanism, in which  $\text{O}_2\text{NOO}^-$  decomposition proceeds without participation of **11b**. We cannot conclusively state based on thermodynamics alone that **11b** is an important participant, however we do note that the rate constant for relaxation of  ${}^1\text{O}_2$  to  ${}^3\text{O}_2$  in water is a reasonably fast process ( $2.4\text{--}3.2 \times 10^5 \text{ s}^{-1}$ ),<sup>28a–f</sup> that should be competitive with the second-order reaction of  ${}^1\text{O}_2$  with nitrite in water ( $3.1 \times 10^6 \text{ L mol}^{-1} \text{ s}^{-1}$ ),<sup>28g</sup> barring the influence of cage effects which might enhance back-reaction of the ion/molecule pair. Notably, this second-order rate constant is 3 orders of magnitude smaller than that for  $-\mathbf{10b}$ , which is  $4.5 \pm 1.0 \times 10^9 \text{ L mol}^{-1} \text{ s}^{-1}$ .<sup>6c</sup> Overall, thermodynamic and kinetic data tend to favor Goldstein et al.’s “Mechanism I”, where **11b** is the first elementary kinetic step in  $\text{O}_2\text{NOO}^-$  decomposition.

**Properties of  $\text{NO}_2$  vs  $\text{NO}_3$  Largely Govern the O–O BDEs.** The reason for the large difference in O–O BDEs between PNI and PNA lies with the very different nature of the  $\text{NO}_2$  and  $\text{NO}_3$  radicals. One way to evaluate this difference is in terms of “reorganization energy”. McKee has pointed out that bond formation between  $\text{NO}_2$  and  $\text{X}^\bullet$  to give  $\text{ONO-X}$  species is a process which necessarily involves deformation of the delocalized radical toward a hypothetical localized  $\text{O=N-O}^\bullet$  isomer.<sup>19</sup> In this process, one N–O bond shortens, becoming closer to a full double bond, while the other lengthens, becoming closer to a single bond. Formation of a new O–X bond requires

- (25) (a) Wenthold, P. G.; Squires, R. S. *J. Phys. Chem.* **1995**, *99*, 2003. (b) Chang, D. P.; Ng, C. Y. *J. Chem. Phys.* **1993**, *98*, 759. (c) Becke, A. J. *Chem. Phys.* **1992**, *97*, 9173. (d) Grev, R. S.; Schaefer, H. F. *J. Chem. Phys.* **1992**, *97*, 8389.
- (26) (a) Khan, A. U.; Kovacic, D.; Kolbanovsky, A.; Desai, M.; Frenkel, K.; Geacintov, N. E. *Proc. Natl. Acad. Sci. USA* **2000**, *97*, 2984. (b) Merényi, G.; Lind, J.; Czapski, G.; Goldstein, S. *Proc. Natl. Acad. Sci. USA* **2000**, *97*, 8216.

(27) Goldstein, S.; Czapski, G.; Lind, J.; Merényi, G. *J. Phys. Chem. A* **1999**, *103*, 3136–3137.

(28) (a) Studer, S. L.; Brewer, W. E.; Martinez, M. L.; Chou, P.-T. *J. Am. Chem. Soc.* **1989**, *111*, 7643. (b) Schmidt, R. *J. Am. Chem. Soc.* **1989**, *111*, 6983. (c) Egorov, S. Y.; Kamalov, V. F.; Koroteev, N. I.; Krasnovsky, A. A.; Toleutaev, B. N.; Zinukov, S. V. *Chem. Phys. Lett.* **1989**, *163*, 421. (d) Chou, P.-T.; Khan, S.; Frei, H. *Chem. Phys. Lett.* **1986**, *129*, 463. (e) Parker, J. G.; Stanbro, W. D. *J. Photochem.* **1984**, *25*, 545. (f) Rodgers, M. A. J. *J. Am. Chem. Soc.* **1983**, *105*, 6201. (g) Bilski, P.; Szychlinski, J.; Oleksy, E. *J. Photochem. Photobiol., A* **1988**, *45*, 269.

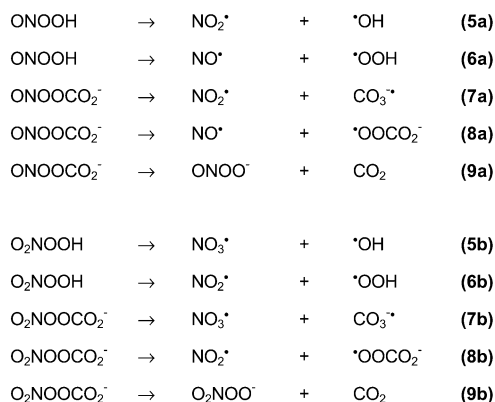


**Figure 2.** Summary of bond homolysis and heterolysis reactions of  $\text{O}_x\text{-NOOR}$  ( $x = 1$  or  $2$ ,  $\text{R} = \text{H}$  or  $\text{CO}_2^-$ ), computed by CBS-QB3 theory.

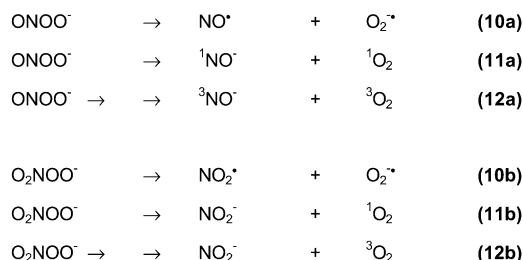


**Figure 3.** Summary of central N–O bond homolysis and heterolysis reactions of  $\text{O}_x\text{NOO}^{\bullet}$  ( $x = 1$  or  $2$ ), computed by CBS-QB3 theory.

the unpaired spin to localize completely on one oxygen atom, thereby sacrificing the energy benefit of delocalization. In the case of  $\text{NO}_2$ , such deformation involves a large “reorganization energy” penalty, which results in a relatively weak  $\text{ONO-X}$  bond. Using thermochemical data for several  $\text{ONO-X}$  species ( $\text{X} = \text{H}, \text{CH}_3, \text{F}, \text{Cl}$ ), McKee obtained an experimental reorganization energy for  $\text{NO}_2$  of  $28 \pm 4$  kcal/mol.<sup>19</sup> A similar approach can be applied to  $\text{NO}_3$ , which must also localize the unpaired spin on one oxygen atom to form an  $\text{O}_2\text{NO-X}$  bond. From thermochemical data<sup>29</sup> for several  $\text{O}_2\text{NO-X}$  species ( $\text{X} = \text{H}, \text{CH}_3, \text{CH}_2\text{CH}_3, \text{F}$ ), we can estimate an experimental reorganization energy for  $\text{NO}_3$  of only  $7 \pm 5$  kcal/mol.

Using a series of constrained optimizations, comparative reorganization energy profiles can be obtained theoretically, by stretching one N–O bond of  $\text{NO}_2$  or  $\text{NO}_3$  from the equilibrium lengths (Figure 4). This is a simple mimic of the process that  $\text{NO}_2$  and  $\text{NO}_3$  must undergo when forming (or breaking) a  $\text{ONO-X}$  or  $\text{O}_2\text{NO-X}$  bond. As expected, the unpaired spin localizes on the oxygen of the “stretched” N–O bond in both cases. Note the significantly steeper curve for  $\text{NO}_2$  than  $\text{NO}_3$ . At the UB3LYP/CBSB7 level of theory, the equilibrium  $\text{O}_x\text{N-OOH}$  bond lengths are 1.390 Å (*syn*-ONOOH) or 1.411 Å (*anti*-ONOOH) and 1.529 Å ( $\text{O}_2\text{NOOH}$ ), respectively. Taking these points on the curves in Figure 4, the computed reorganization energies are 17.3–19.9 kcal/mol for  $\text{NO}_2$  and 10.5 kcal/mol for  $\text{NO}_3$ . Thus theoretical reorganization energies for  $\text{NO}_2$  and  $\text{NO}_3$  reacting with OH to form PNI or PNA agree reasonably well with experimental reorganization energies.

(29) Thermochemical data used for this purpose were taken from the *NIST WebBook* (<http://webbook.nist.gov>). The same method for estimating the  $\text{NO}_2$  reorganization energy used by McKee (see ref 19, Table 7) was used. For consistency, the same “standard” BDE’s for O–H, O–F, and O–C bonds used in ref 19 were also used here.

### Energetic Penalty of N–O Single Bond Distortion in $\text{NO}_2$ and $\text{NO}_3$ Radicals

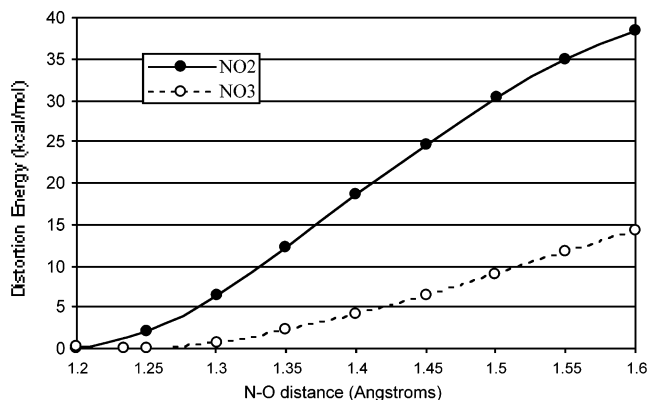


**Figure 4.** Results of constrained optimizations of  $\text{NO}_2^{\bullet}$  and  $\text{NO}_3^{\bullet}$ . CBS-QB3 relative energy (kcal/mol) versus N–O bond distance (Å).

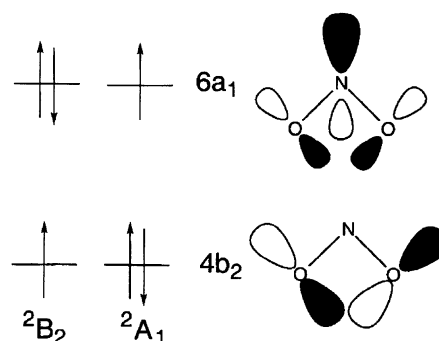


**Figure 5.**  ${}^2\text{B}_2$  excited state of  $\text{NO}_2$  is an O-centered radical, 17–25 kcal/mol higher in energy than the  ${}^2\text{A}_1$  ground state, which is an N-centered radical. In the  ${}^2\text{B}_2$  state, the  $6a_1$  orbital is doubly occupied, whereas in the  ${}^2\text{A}_1$  state the  $4b_2$  orbital is doubly occupied. A doubly occupied orbital will have a stronger effect on the geometry than a singly occupied orbital. So because the  $6a_1$  orbital has an attractive O–O interaction, while the  $4b_2$  orbital has a repulsive O–O interaction, the  $\text{ONO}$  angle in  ${}^2\text{B}_2$   $\text{NO}_2$  is smaller ( $102^\circ$ ) than in  ${}^2\text{A}_1$   $\text{NO}_2$  ( $\sim 134^\circ$ ).

A more fundamental way to understand these differences between PNI and PNA derivatives is to consider the electronic state of the constituent radical fragments. In an  $\text{ONO-X}$  species, the  $\text{NO}_2$  fragment is formally in the  ${}^2\text{B}_2$  excited state, which is an O-centered radical (Figure 5).

The  ${}^2\text{B}_2$  state of  $\text{NO}_2$  is 17–25 kcal/mol higher in energy than the  ${}^2\text{A}_1$  ground state, which is an N-centered radical (Figure 5, top).<sup>30</sup> With breakage of the  $\text{ONO-X}$  bond, relaxation of  $\text{NO}_2$  to the  ${}^2\text{A}_1$  ground state can occur. Hence, the BDE is relatively low. Similar to  $\text{NO}_2$ , the  $\text{NO}_3$  fragment in an  $\text{O}_2\text{NO-X}$  molecule is also formally bound in a  ${}^2\text{B}_2$  state. But breakage of the  $\text{O}_2\text{NO-X}$  bond does not occur with relaxation of the radical to a lower-energy state. It is true that in  $D_{3h}$  symmetry, the  $\text{NO}_3$  radical is  ${}^2\text{A}_2$ ; however, this is similar to the  ${}^2\text{B}_2$  state (Figure 6).

Furthermore, detailed molecular orbital studies of the minimum energy structure of  $\text{NO}_3$  indicate at best a weak preference for  $D_{3h}$  symmetry.<sup>31</sup> If dynamic symmetry-averaging processes

(30) (a) Blahous, C. P.; Yates, B. F.; Xie Y.; Schaefer H. F. *J. Phys. Chem.* **1990**, *93*, 8105. (b) Kaldor, U. *Chem. Phys. Lett.* **1991**, *185*, 131. (c) Jackels, C. F.; Davidson, E. R. *J. Chem. Phys.* **1976**, *64*, 2908. (d) Jackels, C. F.; Davidson, E. R. *J. Chem. Phys.* **1976**, *65*, 2941. (31) (a) Davy, R. D.; Schaefer, H. F. *J. Chem. Phys.* **1989**, *91*, 4410. (b) Kaldor, U. *Chem. Phys. Lett.* **1991**, *185*, 131. (c) Stanton, J. F.; Gauss, J.; Bartlett, R. J. *J. Chem. Phys.* **1991**, *94*, 4084. (d) Stanton, J. F.; Gauss, J.; Bartlett, R. J. *J. Chem. Phys.* **1992**, *97*, 5554. (e) Monks, P. S.; Stief, L. J.; Krauss,

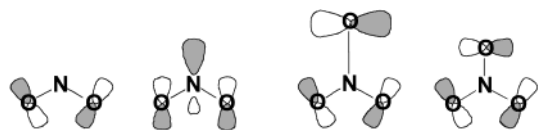


**Figure 6.** Comparison of SOMOs for (left to right)  ${}^2B_2$  excited-state  $\text{NO}_2$ ,  ${}^2A_1$  ground-state  $\text{NO}_2$ ,  ${}^2B_2$  distorted ground-state  $\text{NO}_3$ , and  ${}^2A_2$  ground-state  $\text{NO}_3$ .  $\text{ONO-X}$  species can be considered as having the  $\text{NO}_2$  fragment bound as an O-centered  ${}^2B_2$  radical, which can relax to the N-centered  ${}^2A_1$  radical when the O-X bond homolyzes. When the O-X bond of an  $\text{O}_2\text{-NO-X}$  species homolyzes, the  ${}^2B_2$  O-centered radical undergoes more modest relaxation, either to a less distorted  ${}^2B_2$  state or to a higher-symmetry but energetically similar  ${}^2A_2$  state, but remains an O-centered radical.

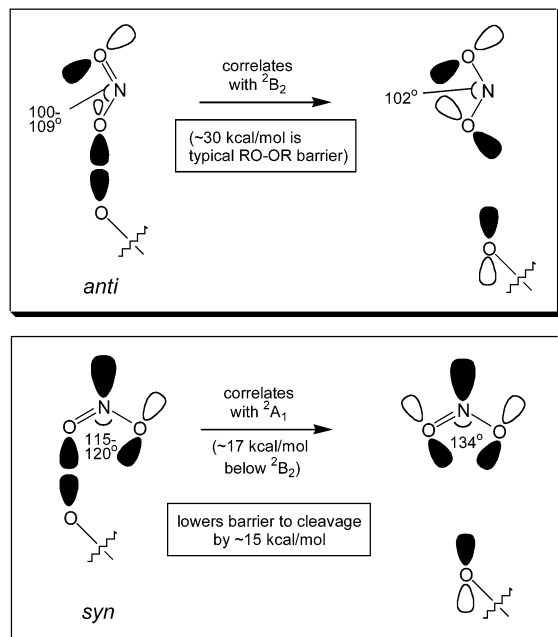


**Figure 7.** Depiction of how O-O bond breaking in ONOOH and perhaps other peroxy nitrite derivatives correlates in a conformation-dependent fashion with either the  ${}^2B_2$  excited state (in the case of a *anti*-ONOOH moiety; top) or the  ${}^2A_1$  ground state (in the case of a *syn*-ONOOH moiety; bottom) of the departing  $\text{NO}_2$  fragment. This may be a result of steric effects, orbital overlap effects, or both.

are ignored, a structure deformed to  $C_{2v}$  symmetry with one long N-O bond and the unpaired spin relatively localized on the unique oxygen, might even be slightly favored.<sup>30c</sup> Because an  $\text{NO}_3$  fragment in  $\text{O}_2\text{NO-X}$  is in an electronic state that is virtually degenerate in energy as that of free  $\text{NO}_3$ , the bond does not homolyze very readily.

Interestingly, the conformational isomers *syn*- and *anti*-ONOOH may differ in how O-O bond breaking responds to the  ${}^2B_2 \rightarrow {}^2A_1$  state change (Figure 7).

We cannot locate a true saddle point for O-O homolysis, however calculations (e.g., a broken symmetry UB3LYP/CBSB7 singlet state) where the O-O distance is increased stepwise reveal that  $\text{NO}_2$  from *syn*-ONOOH correlates with the  ${}^2A_1$  state, (ONO angle =  $129^\circ$  at an O-O distance of 2.15 Å) and smoothly dissociates to  $\text{HO} + \text{NO}_2$ . On the other hand,  $\text{NO}_2$  from *anti*-ONOOH correlates with the  ${}^2B_2$  state (ONO angle =  $102^\circ$  at an O-O distance of 3.25 Å) and the energy of the radical pair rises far more steeply. A possible explanation is that steric effects in the *syn* conformation widen the ONO angle, thereby favoring the  ${}^2A_1$  state, whereas the lack of such effects

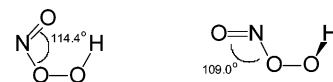
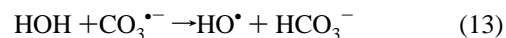


**Figure 8.** Comparison of B3LYP/CBSB7 O-N-O bond angles for *syn*-ONOOH and *anti*-ONOOH. Steric effects and/or orbital overlap effects result in a larger angle for the *syn* conformation, and favor correlation with the  ${}^2A_1$  ground state. This results in more facile O-O bond breaking than in the *anti* conformation (although this does not show up in thermodynamic calculations, because the products are the same in either case and *anti*-ONOOH is the less stable conformation by 3.1 kcal/mol at the CBS-QB3 level).

in a *anti* conformation results in a smaller ONO angle, hence correlating better with the  ${}^2B_2$  excited state (Figure 8).

There might also be other, more complex explanations related to orbital overlap. Regardless of the starting conformation, the  $\text{NO}_2$  radical that forms should ultimately relax to the  ${}^2A_1$  state, so the “equilibrium” BDE for *anti*-ONOOH is actually lower because the *anti* isomer is 3.1 kcal/mol higher in energy conformation than *syn*-ONOOH.

The structure of the other radical fragment also influences the O-O BDEs. For example, better stabilization of the unpaired spin is expected in carbonate radical than hydroxy radical, which is an important factor for the dramatic instability of PNI in the presence of  $\text{CO}_2$ . Reaction **7a**, which yields carbonate radical, is 12.2 kcal/mol less endothermic than **5a**, which yields hydroxyl radical. This difference is less pronounced in PNA, as **7b** is only 5.8 kcal/mol less endothermic than **5b**. It seems that the maximum effect is not fully realized in either the PNI or PNA case: at the CBS-QB3 level, the isodesmic reaction **13** lies 27.4 kcal/mol to the left



Other factors may be involved as well. For example, stronger electron-withdrawing effects in  $\text{O}_2\text{NOOCO}_2^-$  might result in more ground-state stabilization compared to  $\text{ONOOCO}_2^-$ , thereby raising all BDE of the PNA  $\text{CO}_2$  adduct.

**Further Comparison of Theory and Experiment.** Experimental estimates place the two-electron reduction potentials of  $\text{O}_2\text{NOOH}$  and  $\text{ONOOH}$  at 1.83 and 1.68 V (vs NHE), respectively.<sup>6</sup> On this basis alone,  $\text{O}_2\text{NOOH}$  is predicted to be a thermodynamically more potent oxidant than is  $\text{ONOOH}$ . Our calculations indicate that oxygen atom transfer from PNA to amines, sulfides, and alkenes may be more facile in some, but not all cases, as compared to when PNI is the oxygen donor.<sup>12</sup> However, the activation barriers for these processes are quite similar, such that any preference might be either reinforced or counteracted by specific solvent and/or ion effects.

The computed O-O BDEs of  $\text{O}_x\text{NOOR}$  ( $x = 1$  or  $2$ ,  $\text{R} = \text{H}$  or  $\text{CO}_2^-$ ) are consistent with experimental observations. PNA is more stable than PNI at low pH, where the  $\text{O}_x\text{NOOH}$  forms predominate ( $\text{HOONO}$   $\text{p}K_a = 6.8$ ;  $\text{HOONO}_2$   $\text{p}K_a = 5.9 \pm 0.1$ )<sup>1c,5</sup> The ca. 20 kcal/mol higher O-O BDE which is computed for  $\text{O}_2\text{NOOH}$  relative to  $\text{ONOOH}$  is in excellent agreement with the experimental value.<sup>6b,c,8</sup> Likewise, our computations and others in the literature<sup>11</sup> indicate that the central N-O bond of  $\text{O}_2\text{NOOH}$  is weaker than the O-O bond, and therefore agree with the observation that the products of homolysis of  $\text{O}_2\text{NOOH}$  are  $\text{OOH} + \text{NO}_2$ , rather than  $\text{OH} + \text{NO}_3$ .<sup>8,6b</sup> Our calculations also indicate that the O-O bond of  $\text{O}_2\text{NOOCO}_2^-$  is about 20 kcal/mol stronger than that of  $\text{ONOOCO}_2^-$ . This is in accord with the observation that PNI

M.; Kuo, S. C.; Zhang, Z.; Klemm, R. B. *J. Phys. Chem.* **1994**, *98*, 10 017.

readily decomposes in the presence of  $\text{CO}_2$ ,<sup>9</sup> whereas PNA is not sensitive to the presence of  $\text{CO}_2$ .<sup>4</sup> It now seems generally accepted that  $\text{ONOOH}$  and  $\text{ONOOCO}_2^-$  homolyze readily to give the  $\text{NO}_2/\text{HO}$  or  $\text{NO}_2/\text{CO}_3^-$  radical pairs.<sup>7,10</sup> No similar observations have been reported for PNA,<sup>4,10</sup> in fact PNA appears to be quite insensitive to the presence of  $\text{CO}_2$ . We expect that  $\text{O}_2\text{NOOCO}_2^-$  should form, but our calculations suggest decarboxylation probably occurs to regenerate  $\text{O}_2\text{NOO}^- + \text{CO}_2$  (reaction **9b**).

## Conclusions

We find that PNA and PNI have similar barriers for O-atom transfer reactions to heteroatoms and double bonds. The transition states for these reactions are similar to those previously published for oxidations by PNI and other peracids.

Unlike the O-atom transfer reactions, the O–O BDEs of  $\text{O}_x\text{-NOOR}$  ( $x = 1$  or  $2$ ,  $\text{R} = \text{H}$  or  $\text{CO}_2^-$ ) differ very significantly. The  $\text{CO}_2$  adducts have significantly lower BDEs than the parent acids, because a carbonate radical has a better-stabilized unpaired electron than a hydroxy radical. The much lower BDEs of  $\text{ONOOR}$  than  $\text{O}_2\text{NOOR}$  species can be explained either in terms of the much larger “reorganization energy” of  $\text{NO}_2$  than  $\text{NO}_3$ , or more fundamentally as an  $\text{NO}_2$  radical fragment shifting from the excited ( $^2\text{B}_2$ ) state with the unpaired electron centered on O to the ground ( $^2\text{A}_1$ ) state with the unpaired electron centered on N. No comparable change from the ground state to the excited state occurs with  $\text{NO}_3$ , which simply remains an O-centered radical. For these reasons, unlike  $\text{ONOOH}$ , unimolecular decomposition of  $\text{O}_2\text{NOOH}$  is not a source of hydroxyl radical.

In the absence of trapping agents such as SOD, N–O bond cleavage in  $\text{ONOO}^-$  is likely to be largely unproductive because there is no thermodynamic sink that is readily accessible to the products, as there is in the case of  $\text{O}_2\text{NOO}^-$  (i.e., nitrite + triplet oxygen). Thus other, more complex pathways for  $\text{ONOO}^-$  decomposition are followed.

The calculations show that  $\text{O}_2\text{NOO}^-$  can readily self-decompose by N–O bond breakage (reaction **10b** and/or **11b**) because eventual formation of nitrite and triplet oxygen is thermodynamically favorable with respect to starting material. This difference is due to nitrite formation being more favorable than formation of nitroxyl anion. Although the N–O heterolysis reaction of  $\text{O}_2\text{NOO}^-$  (reaction **11b**) should be strongly favored over homolysis (reaction **10b**) in the gas phase, this preference is significantly reduced in water because solvation of superoxide is predicted to be ca. 12 kcal/mol more favorable than solvation of nitrite. In water, both pathways might have similar forward rate constants, but **–10b** should be much faster than **–11b**, which would be in agreement with the first of two previously proposed mechanisms<sup>6c</sup> for  $\text{O}_2\text{NOO}^-$  decomposition.

**Acknowledgment.** We are grateful to the National Science Foundation and the National Institute of General Medical Sciences, National Institutes of Health, for financial support of this research. M.D.B. acknowledges the support of the National Research Service Award, National Institutes of Health.

JA029619M